The EMBO Journal Vol.17 No.4 pp.977–984, 1998

Synapsin I is structurally similar to ATP-utilizing enzymes

Lothar Esser, Chyung-Ru Wang[1], Masahiro Hosaka[2], Cynthia S.Smagula[3], Thomas C.Südhof[2] and Johann Deisenhofer[4]

Howard Hughes Medical Institute and Department of Biochemistry and [2]Howard Hughes Medical Institute and Department of Molecular Genetics, University of Texas Southwestern Medical Center, 5323 Harry Hines Blvd, Dallas, TX 75235-9050, USA

[1]Present address: Department of Pathology, Committee of Immunology, Gwen Knapp Center for Lupus and Immunology Research, University of Chicago, Chicago, IL 60637-5420, USA
[3]Present address: Biota Publications, P.O. Box 801082, Dallas, TX 75380-1082, USA

[4]Corresponding author
e-mail: jd@howie.swmed.edu

Synapsins are abundant synaptic vesicle proteins with an essential regulatory function in the nerve terminal. We determined the crystal structure of a fragment (synC) consisting of residues 110–420 of bovine synapsin I; synC coincides with the large middle domain (C-domain), the most conserved domain of synapsins. SynC molecules are folded into compact domains and form closely associated dimers. SynC monomers are strikingly similar in structure to a family of ATP-utilizing enzymes, which includes glutathione synthetase and D-alanine:D-alanine ligase. SynC binds ATP in a Ca^{2+}-dependent manner. The crystal structure of synC in complex with ATPγS and Ca^{2+} explains the preference of synC for Ca^{2+} over Mg^{2+}. Our results suggest that synapsins may also be ATP-utilizing enzymes.

Keywords: ATP binding/Ca^{2+} binding/crystal structure/structural similarity/synaptic vesicle proteins

Introduction

Synapsins account for ~9% of the proteins associated with synaptic vesicle membranes, and occur in two major forms (synapsin I and II), each of which in turn is found in two isoforms (Ia and Ib, IIa and IIb) (Greengard, 1987; Südhof *et al.*, 1989; Rosahl *et al.*, 1993, 1995; Südhof, 1995; Klagges *et al.*, 1996). They are phosphorylated by multiple kinases (Greengard, 1987; Südhof, 1995). *In vitro* binding studies revealed a bewildering variety of proteins that specifically interact with synapsins. These include major elements of the cytoskeleton [actin microfilaments, neurofilaments, microtubuli and spectrin (Baines and Bennett, 1985, 1986; Bähler and Greengard, 1987; Steiner *et al.*, 1987; Petrucci and Morrow, 1997)], of which binding to microfilaments and neurofilaments is regulated by phosphorylation. In addition, synapsin I binds calmodulin and annexin VI in a Ca^{2+}-dependent manner (Hayes *et al.*, 1991; Inui *et al.*, 1994) and the MARCKS protein and Grb2 independently of Ca^{2+} (Mizutani *et al.*, 1992; McPherson *et al.*, 1994). Nerve terminal functions are maintained in the absence of synapsins in mice but are severely impaired. This suggests that synapsins have an important role in maintaining regulated vesicular traffic, although they are not essential for membrane traffic as such (Rosahl *et al.*, 1995). The exact function of synapsins has remained obscure.

Synapsins Ia (706 amino acids) and Ib (670 amino acids) are derived from one gene by differential splicing of the mRNA and differ from each other only at their carboxy-termini. Synapsin I is composed of a globular amino-terminal region and a proline-rich, elongated and basic carboxy-terminal region. The primary structure is 95% conserved between rat, bovine (Südhof *et al.*, 1989) and human forms; it contains five domains (A, B, C, D and E/F) distinguishable on the basis of composition and degree of evolutionary conservation. Of these, the central 'C' domain is the most highly conserved and is contained within the amino-terminal globular region of synapsin known to be resistant to collagenase digestion. Here we report the three-dimensional structure of the recombinant C domain (synC, amino acids 110–420) of bovine synapsin I and of its complex with ATPγS and Ca^{2+}.

Results

Structure of synC

We determined the crystal structure of synC and refined the atomic model at 2.15 Å resolution. As shown in Figure 1A and C, synC forms a compact structure with roughly elliptical shape; the amino and carboxyl ends of the domain are near one of its tips, only 15 Å apart. Surprisingly, the three-dimensional alignment (DALI; Holm and Sander, 1993) of synC with the structures deposited in the Brookhaven protein data bank (PDB; Bernstein *et al.*, 1977) revealed strong architectural similarities to the following enzymes: glutathione synthetase (GSHase; Yamaguchi *et al.*, 1993), D-alanine:D-alanine ligase (ddligase; Fan *et al.*, 1994), biotin carboxylase α-chain (BNC; Waldrop *et al.*, 1994), succinyl CoA synthetase β-chain (SCS; Wolodko *et al.*, 1994) and pyruvate, orthophosphate dikinase (PPDK; Herzberg *et al.*, 1996). All these enzymes catalyze similar types of reactions, which include the transfer of phosphate from bound ATP to a substrate (Artymiuk *et al.*, 1996; Matsuda *et al.*, 1996). The striking resemblance between synC and GSHase is apparent from Figure 1A and B. More than 80% of the Cα atoms of synC can be superimposed onto those of the two top-scoring molecules, GSHase and ddligase, with a root-mean-square deviation (r.m.s.d.) of 3.2 Å each, without any permutation of topological connections. Thus, synC shares a common fold with

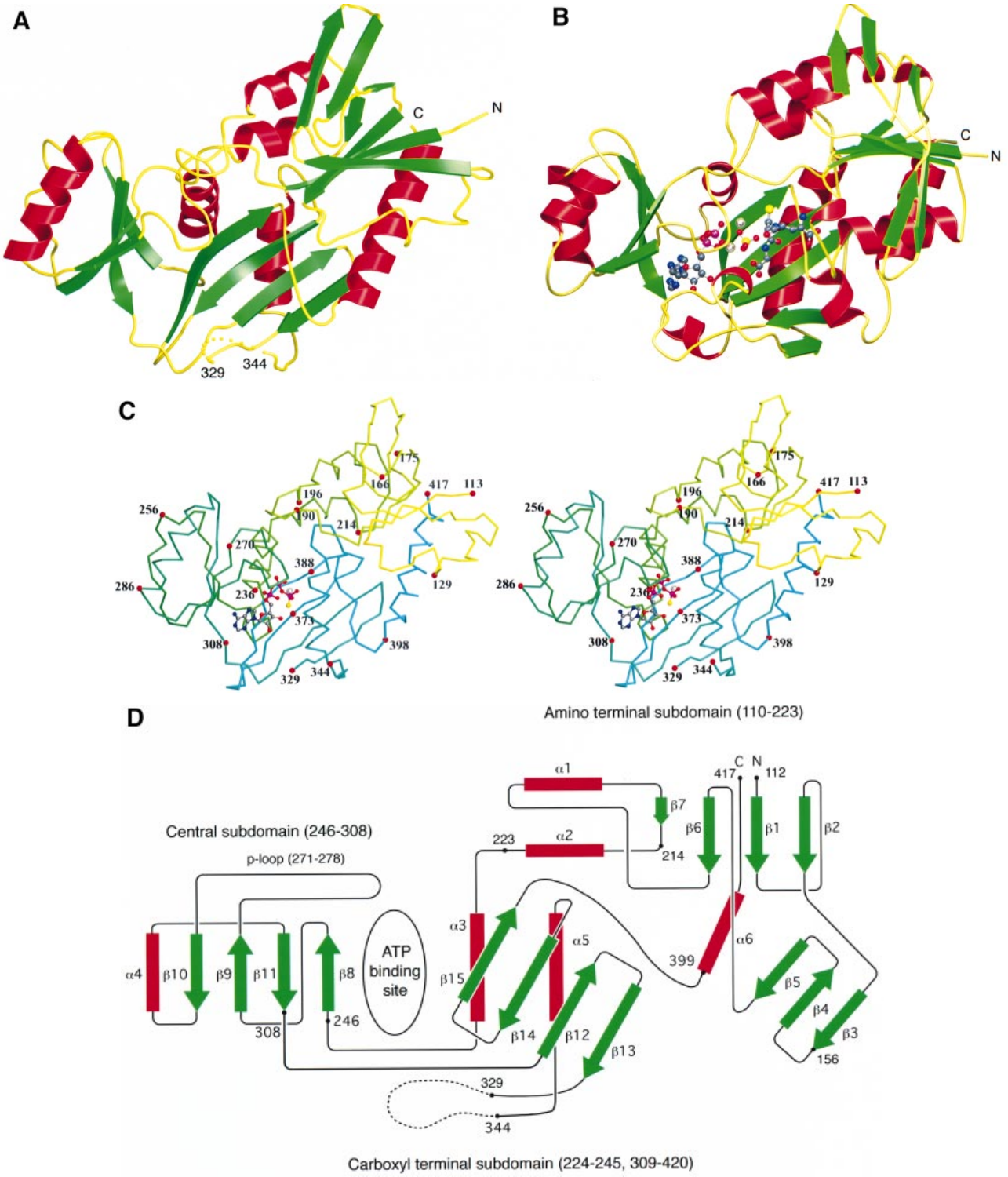

Fig. 1. Ribbon diagrams of the monomers of (**A**) synC and (**B**) the complex of glutathione synthetase with MgADP and glutathione as ball-and-stick models (PDB entry 1gsa). (**C**) Stereo drawing of the Cα-trace of synC, colored yellow to blue from the amino- to the carboxy-terminus; a ball-and stick model in atom colors of bound ATPγS is also shown. Selected Cα-atoms are marked with red balls and residue numbers. (**D**) Topology diagram of synC. Disordered residues are indicated by dotted lines. (A), (B) and Figure 4 were made with a modified version of the program Molscript (Esnouf, 1997).

members of a superfamily of enzymes which have been classified as α and β structures (SCOP; Murzin *et al.*, 1995). Because of the low sequence identity (9–14%) between members of this superfamily, including synC, the similarity could not be detected in the absence of three-dimensional structures.

The structure of synC can be divided into three subdomains (Figure 1D): the amino-terminal subdomain

(residues 110–223), the central subdomain (residues 246–308) and the carboxy-terminal subdomain (residues 224–245 and 309–420). The core of the amino-terminal subdomain is a four-stranded parallel β-sheet (β1, β2, β6, β7), which is flanked by a helical loop (residues 124–137) and helix α1. It resembles the nucleotide-binding motif (NAD motif) found in numerous enzymes that bind substrates at the carboxyl end of the parallel β-sheet. The parallel arrangement of helices α1 and α2 and their connection by strand β7 are remarkably well conserved in synC and GSHase. Even more remarkable is the existence of a *cis*-asparagine residue at the carboxyl end of strand β7 in both synC (Asn214) and GSHase (Asn114). As the *cis* conformation is extremely rare in peptide bonds preceding residues other than proline, the use of *cis*-asparagine at equivalent positions in synC and GSHase makes the similarity between the two proteins even more compelling.

The central subdomain is characterized by a four-stranded antiparallel β-sheet and contains a glycine-rich loop between strands β9 and β10 which can be superimposed with loops in GSHase (residues 162–169) and ddligase (residues 146–153). The crystal structures of the nucleotide complexes of GSHase and ddligase revealed that these loops bind to the β-phosphate of the nucleotide (p-loop). Thus, the central subdomain of synC has the ATP grasp motif (Murzin *et al.*, 1995) which is the most prominent common feature of all members of this superfamily of ATP-binding enzymes.

A large antiparallel β-sheet in the carboxy-terminal subdomain, comprising strands β13–β15 in synC, is also common to these enzymes. The antiparallel β-sheets of the central and carboxy-terminal subdomains are facing each other and form a cavity large enough to accommodate both ATP and a putative substrate. Within the carboxy-terminal subdomain of synC, the polypeptide chain between residues 330 and 343 is disordered in the crystal. According to structural superposition, the disordered residues of synC are equivalent to the multifunctional loop (residues 226–242) in GSHase. In the structure of the apo form of GSHase (PDB entry 2glt), this loop is disordered, but assumes a fixed conformation in the crystal structure of the complex of GSHase with ADP, magnesium ions and glutathione (PDB entry 1gsa). A basic residue within this loop (Arg233) is of crucial importance for the function of GSHase (Tanaka *et al.*, 1992); a comparable basic residue, Lys336, occurs in the sequence of synC. Therefore, by analogy, we infer that these disordered residues in synC belong to a loop whose function requires a high degree of flexibility, and which may become ordered after binding of a suitable ligand to synC. The carboxy-terminal helix α6 is connected to strand β15 by a continuous loop and lies below the amino-terminal domain.

Ca^{2+}-dependent ATP binding

The unexpected similarity of synC to ATP-utilizing enzymes prompted us to test if synC binds ATP, using a GST–synC fusion protein and ATPγS, a non-hydrolyzable ATP analog (Figure 2). We observed robust ATPγS binding that was completely inhibited by ATP with a half-maximum inhibition of 0.14 μM, suggesting a high-affinity ATP-binding site. In contrast, GTP was unable to compete, and fusions of GST with five other proteins failed to bind ATP, demonstrating that binding is specific (data not shown). Surprisingly, ATPγS binding to synapsin I was completely dependent on Ca^{2+}; no binding could be observed in the absence of Ca^{2+} (Figure 2). We confirmed these results with recombinant full-length synapsin Ia produced in a baculovirus expression system, and with ATP instead of ATPγS (not shown).

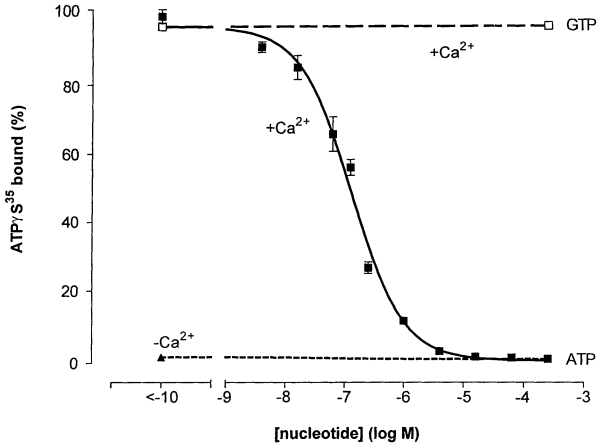

Fig. 2. ATP binding by the recombinant C-domain of synapsin I. ^{35}S-Labeled ATPγS bound to GST–synapsin I C-domain fusion protein (50 nM protein) was measured in the presence or absence of Ca^{2+} and of increasing concentrations of ATP and GTP. The half-maximum inhibition of ATPγS binding occurs at 0.14 μM ATP.

To understand the structural basis for Ca^{2+}-dependent, specific, high-affinity ATP binding by synC, we investigated the crystal structure of a complex between ATPγS and synC (CaATPγS). This structure revealed a single Ca^{2+} ion, coordinated by Glu373, Glu386 and the pyrophosphate moiety of ATPγS (Figure 3A and B). Calcium–oxygen bond distances between 2.4 and 3.0 Å were in the range of values expected for a Ca^{2+} ion with a coordination number of six (Falke *et al.*, 1994). However, the high average temperature factor of the triphosphate group (B = 83 Å^2) defied an exact description of its conformation and hapticity. Still, the position of the Ca^{2+} ion was unambiguous due to the coordination of Glu373 and Glu386 which anchor it in a central position between the pyrophosphate of ATPγS and strands β14 and β15. The binding of ATPγS and Ca^{2+} did not cause detectable movements of the subdomains of synC.

In GSHase and ddligase, two magnesium ions interact with the nucleotide and are believed to facilitate the nucleophilic attack on the γ-phosphate of ATP by balancing the negative charges on the pyrophosphate and to help stabilize the acylphosphate intermediate. Most of the catalytic residues in GSHase and ddligase, in particular the ones that interact with ATP and Mg^{2+} ions, are well conserved in synC (Figure 3B and C, Table I). An exception is the polar residue Asn283 in GSHase (Asn272 in ddligase) which coincides with the hydrophobic residue Val388 in synC. Residue Asn283, together with Glu281, coordinates magnesium ion Mg2 in the active site of GSHase (and in that of ddligase) (Figure 3C). The substitution of Val for Asn at residue 388 in synC prevents the stabilization of a metal ion in an equivalent position. In GSHase, the magnesium ion Mg1 is coordinated primarily by the α- and β-phosphate groups as well as a sulfate ion that mimics the detached γ-phosphate after the reaction

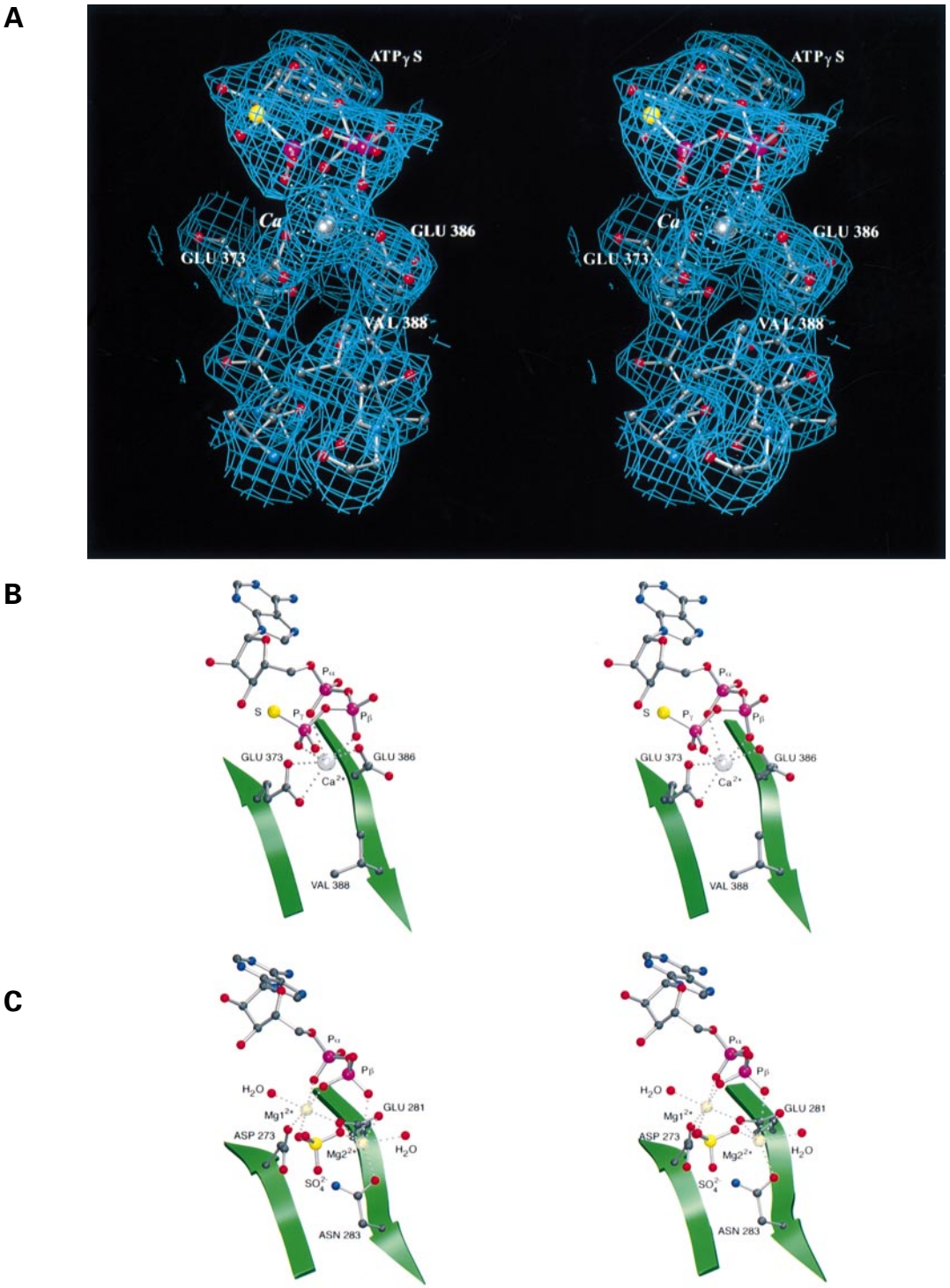

Fig. 3. Stereo pairs of the metal-binding sites in CaATPγS (**A** and **B**) and in GSHase (**C**). (A) Electron density and ball-and-stick model around the Ca^{2+}-binding site [$2F_o$–F_c map at 2.3 Å resolution after refinement; contour level 1σ (electron density)]. (B) and (C) were made with the program Molscript (Kraulis, 1991) and rendered in povray 3.0.

occurred (Figure 3C). Ca^{2+} in CaATPγS occupies a position roughly equivalent to Mg1 in GSHase. The involvement of Ca^{2+} in ATP binding has also been observed in the ATPase domains of bovine 70 kDa heat shock cognate protein (Flaherty *et al.*, 1994) and human 70 kDa heat shock protein (Sriram *et al.*, 1997). Both these enzymes undergo Ca^{2+}-dependent autophosphorylation *in vitro*, indicating that ATP hydrolysis in the presence of Ca^{2+} is possible, and that it could also occur in synapsin I.

The synC dimer

In the crystal, two molecules of synC form a tight dimer around a crystallographic 2-fold axis (Figure 4) with a buried surface area of 1300 Å^2 per monomer; the contacts between these molecules are predominantly hydrophobic. The asymmetric unit of synC crystals contains two molecules related by a 2-fold non-crystallographic symmetry (ncs) axis perpendicular to the tight dimer axis. This arrangement of 2-fold axes generates two kinds of tetra-

Table I. Structurally and possibly functionally equivalent residues in the active site

SynC/Ca-ATPγS	GSHase	ddligase	Function
			Adenosyl moiety of ATP
Lys269	Lys160	Lys144	N7 (ATP), O1 (Pα)
Glu305	Gln198	Glu180	N6 (ATP)
Phe307	Tyr200	Trp182	hydrophobic shield
Ile308	Leu201	Leu183	amide H bond to N1 (ATP)
Asp313	Asp208	Glu187	single or multiple H-bonds to O2*/O3* of ribose
			Phosphate-binding residues
Ser275	Gly166	Ser150	amide H bond to O2 (Pβ)
Gly276	Gly167	Gly151	amide H bond to O2 (Pβ)
Lys225	Lys125	Lys97	near O1 (Pβ)
Lys279	Ile170	Met154	near O1 (Pα), O2 (Pβ)
			Metal-binding residues
Glu373	Asp273	Asp257	η^2 to Ca or η^1 bond to Mg1
Glu386	Glu281	Glu270	η^1 to Ca or η^2 bond to Mg2
Val388	Asn283	Asn272	η^1 bond to Mg2
			Long, flexible loop
Lys336	Arg233	Lys215	Crucial residue for catalysis

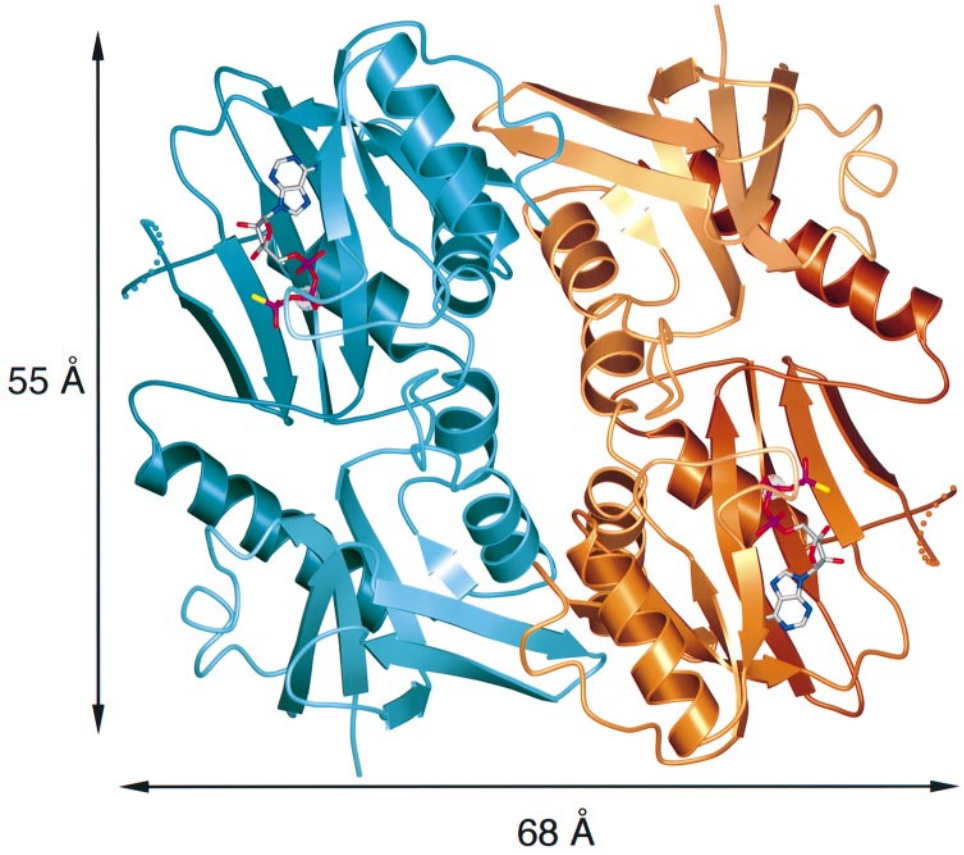

Fig. 4. Schematic drawing of a tight dimer of CaATPγS viewed down the crystallographic 2-fold axis. Monomers are colored blue and brown, with the ligands drawn as ball-and-stick models.

mers of synC with local D_2 point group symmetry. Interactions between ncs-related pairs of synC account for 570 and 330 $Å^2$ of buried surface area, respectively. Because the interaction surface of the tight dimer is much larger and hydrophobic, this dimeric form of synC should be prevalent in solution. Most residues in the tight dimer interface are conserved between synapsins I and II; this suggests that synapsin II can also form dimers, and that even heterodimers of synapsins I and II may exist. Crystals of GSHase contain dimers and tetramers with exact D_2 symmetry (Yamaguchi *et al.*, 1993), very similar to those found in synC crystals.

Discussion

We have found evidence suggesting that the C domain of synapsin (synC) is an ATP-binding protein and, by virtue of its similarity to GSHase, is likely to catalyze the transfer

Table II. Summary of X-ray crystallographic data and analyses

Data collection statistics	Native (SeMet variant)			MeHgCl derivative	Ca^{2+}/ATPγS soak
Data set name	λ_2	λ_3	λ_4	MeHg	CaATPγS
Wavelength [Å]	0.9793	0.9789	0.9686	1.0027	1.5418
f'/f''	–7.35/2.17	–6.2/5.43	–1.07/3.75		
d(min) [Å]	2.15	2.15	2.15	2.35	2.20
Completeness (I>2σI) (%)	74.3	72.6	74.0	85.3	74.9
Measurements	105 390	113 267	107 874	114 695	88 952
Unique reflections	55 873	57 094	56 778	56 486	28 177
R_{merge} (I>–3σI)	0.048	0.053	0.048	0.043	0.054
Refinement statistics	**SYNC (native λ_2)**	**CaATPγS**			
R_{cryst} (%) ($F>0$)	20.12	20.63			
R_{free} (%) ($F>0$)	25.72	26.79			
Resolution range (Å)	30.0–2.15	30.0–2.30			
Anomalous scatterer	20 Se atoms	0			
Water molecules	161	54			
R.m.s.d. bond length (Å)	0.012	0.013			
R.m.s.d. angles (°)	1.55	1.57			
R.m.s.d. improper dihedral angles (°)	1.33	1.41			

of the γ-phosphate of ATP to a substrate whose exact nature remains elusive. There has been one report in the literature suggesting that synapsin I isolated from rat brain might be a diacylglycerol kinase (Kahn and Besterman, 1991), but this result could not be reproduced with recombinant protein (M.Hosaka and T.C.Südhof, unpublished). The amino acid sequence of the C domain of synapsin II is very similar to that of synC (78.6% identity rat synapsin II/bovine synapsin I), but binds mononucleotides without the mediation of divalent cations (M.Hosaka and T.C.Südhof, unpublished). This difference can be explained by a charge inversion of an active site residue: a negatively charged residue (Glu373) that binds to Ca^{2+} in CaATPγS is replaced by a positively charged residue (Lys374) in rat synapsin II and is in an ideal position to bind to the γ-phosphate by way of a salt bridge. The findings described here have revealed an entirely new aspect of the possible function of synapsin and of its role in synaptogenesis and synaptic transmission.

Materials and methods

Binding of ATPγS to synC

GST–synC fusion protein was immobilized on glutathione beads. Beads were washed three times with buffer A (50 mM HEPES-NaOH pH 7.4, 25 mM NaCl, 2mM EGTA with or without 2.1 mM Ca^{2+}). Assays were performed in triplicate using 50 nM GST–synC fusion protein and 10 nM of ^{35}S-labeled ATPγS with the addition of the nucleotides indicated in Figure 2. Controls were performed with GST alone and with fusions of GST with five other proteins. Beads were incubated at 25°C for 1 h, then washed three times with 3 ml of buffer A, and the radioactivity associated with the glutathione beads was counted in a liquid scintillation counter. Data were analyzed by non-linear regression assuming a single binding site, using GraphPad PRISM™ software.

Crystallization

SynC was purified and crystallized as described (Wang *et al.*, 1997). The seleno-methionine variant SeMet-synC was expressed by the methionine auxotroph *Escherichia coli* strain B834/DE3 (Novagen) growing in a medium containing 20 mg/l of L-seleno-methionine. Purification and crystallization were identical to that of wild-type synC except that all buffers contained 10 mM dithiothreitol (DTT) and 5 mM EDTA. Soaking crystals in a cryoprotectant consisting of 30% PEG-4000, 50 mM HEPES (pH 7.5) and 50 mM NaCl for at least 15 h not only preserved the crystal quality during freezing, but also led to crystals with reproducible cell constants. Isomorphous heavy-atom derivatives were obtained by soaking pre-equilibrated crystals in fresh cryoprotectant containing 1 mM MeHgCl and 50 mM HEPES (pH 7.75) for 3–52 h. Similarly, the complex CaATPγS was prepared by treating crystals of synC with cryoprotectant containing 2.5 mM ATPγS and 2.5 mM $CaCl_2$. All crystals were flash-frozen in liquid propane and stored at 77 K.

Data collection

A summary of the X-ray crystallographic data is given in Table II. Diffraction data were collected with a Rigaku R-axis II detector equipped with a rotating anode (Cu) generator, and on Fuji imaging plates at beamline X4a at the Brookhaven National Laboratory. A crystal of the seleno-methionine variant (SeMet-synC) was used to collect three data sets at wavelengths λ_2 = 0.9793 Å, λ_3 = 0.9789 Å and λ_4 = 0.9686 Å corresponding to the inflection point, maximum and a remote point on the EXAFS spectrum at the Se K absorption edge. All data were processed with DENZO, XDisplayF and Scalepack (Otwinowski and Minor, 1997). Crystals of synC and its derivatives/complexes have the symmetry of the trigonal space group $P3_221$ (No. 154) with the respective cell dimensions: $a = b$ = 76.4 Å, c = 180.9 Å (SeMet-synC); $a = b$ = 76.2 Å c = 180.1 Å (MeHg); and $a = b$ = 76.2 Å, c = 182.2 Å (CaATPγS). There are two molecules, related by approximate 2-fold symmetry, in the asymmetric unit.

Phase determination

Difference Patterson techniques in combination with difference Fourier methods revealed the positions of six mercury atoms in MeHg. Sixteen out of 22 possible selenium atoms in SeMet-synC were located by difference Fourier synthesis employing experimental phases from MeHg. Probabilistic phase determination proceeded in MLPHARE (Otwinowski, 1991; Collaborative Computational Project Number 4, 1994) using λ_2 as native reference data set, while data sets λ_3, λ_4 and MeHg served as derivatives. The final figure-of-merit is 0.59 to 2.35 Å resolution. The phases were improved further by 2-fold molecular averaging, solvent flattening and histogram mapping with DM (Collaborative Computational Project Number 4, 1994; Cowtan and Main, 1996).

Model building and refinement

The initial model was built into electron density at 3.0 Å resolution using the program O (Jones *et al.*, 1991). Because the data quality of the seleno-methionine variant exceeded that of any other wild-type synC crystal, our model of synC contains seleno-methionine residues and has been refined against data set λ_2. The SeMet-synC model, containing 292 residues (93.9%), 20 anomalous scatterers (Se) and 161 water molecules, was refined using reflections with $F>0$ between 30.0 and 2.15 Å resolution. The overall completeness of data set λ_2 is 73.4% for the

working set and 8.1% for the cross-validation set. All computations were carried out with X-PLOR 3.851 (Brünger, 1992) and resulted in working and free *R*-factors of 20.2 and 25.7%, respectively. Non-crystallographic symmetry restraints were maintained at all stages of refinement. The deviations of the final model from ideal bond lengths and angles are 0.012 Å and 1.55°, respectively. All residues are in the most favored (92.2%) or additional allowed (7.8%) regions of the Ramachandran diagram.

An initial model of CaATPγS was obtained by refining the coordinates of the synC model against the observed structure factors of the complex. The $2F_o–F_c$ map showed density for one nucleotide and one calcium ion for each monomer. After several cycles of refinement and manual rebuilding, coordinates for two ATPγS molecules, two Ca^{2+} ions and 54 water molecules were included. While the adenosyl moieties of both ATPγS molecules are well defined, the attached pyrophosphate groups are both disordered and were given slightly different conformations. The data quality at the given highest resolution of 2.3 Å did not allow us to resolve the disorder into multiple conformations for each pyrophosphate group. The quality of the geometry of polypeptide chain is similar to that of SeMet-synC with an r.m.s.d. of bond distances and angles from ideal values of 0.013 Å and 1.57°, respectively. All residues are in the most favored (90.5%) or additional allowed (9.5%) regions of the Ramachandran diagram. The crystallographic *R*-factors are 20.6% (working set) and 26.8% (free set) respectively.

In both structures (SeMet-synC and CaATPγS), some residues could not be located due to insufficient electron density. Apart from a total of five missing residues at N- and C-termini, there is a break in the main chain between residues 330 and 343 and only very weak density was present for residues 167–174 and 191–195 which were included in the models but excluded from structure factor calculation by setting their occupancy to zero. The atomic coordinates of SeMet-synC and CaATPγS have been deposited in the Brookhaven Protein Data Bank with accession numbers 1auv and 1aux, respectively.

Acknowledgements

We thank Dr E.Lee for his help with the expression of the selenomethionine variant, M.Palnitkar for her excellent technical assistance and Dr C.Ogata for help with the HHMI beamline X4a at the National Synchrotron Light Source at Brookhaven National Laboratory.

References

Artymiuk,P.J., Poirrette,A.R., Rice,D.W. and Willett,P. (1996) Biotin carboxylase comes into the fold. *Nature Struct. Biol.*, **3**, 128–132.

Bähler,M. and Greengard,P. (1987) Synapsin I bundles F-actin in a phosphorylation-dependent manner. *Nature*, **326**, 704–707.

Baines,A.J. and Bennett,V. (1985) Synapsin I is a spectrin-binding protein immunologically related to erythrocyte protein 4.1. *Nature*, **315**, 410–413.

Baines,A.J. and Bennett,V. (1986) Synapsin I is a microtubule-binding protein. *Nature*, **319**, 145–147.

Bernstein,F.C., Koetzle,T.F., Williams,G.J.B., Meyer,E.F.,Jr, Brice,M.D., Rodgers,J.R., Kennard,O., Shimanouchi,T. and Tasumi,M. (1977) The Protein Data Bank: a computer-based archival file for macromolecular structures. *J. Mol. Biol.*, **112**, 535–542.

Brünger,A.T. (1992) *X-PLOR Version 3.1. A System for X-ray Crystallography and NMR*. Yale University Press, New Haven, CT.

Collaborative Computational Project Number 4, (1994) CCP4. *Acta Crystallogr.*, **D50**, 760–763.

Cowtan,K.D. and Main,P. (1996) Phase combination and cross validation in iterated density-modification calculations. *Acta Crystallogr.*, **D52**, 43–48.

Esnouf,R.M. (1997) An extensively modified version of Molscript that includes greatly enhanced coloring capabilities. *J. Mol. Graph.*, **15**, 133–138.

Falke,J.J., Drake,S.K., Hazard,A.L. and Peersen,O.B. (1994) Molecular tuning of ion binding to calcium signaling proteins. *Q. Rev. Biophys.*, **27**, 219–290.

Fan,C., Moews,P.C., Walsh,C.T. and Knox,J.R. (1994) Vancomycin resistance: structure of D-alanine:D-alanine ligase at 2.3 Å resolution. *Science*, **266**, 439–443.

Flaherty,K.M., Wilbanks,S.M., DeLuca-Flaherty,C. and McKay,D.B. (1994) Structural basis of the 70-kilodalton heat shock cognate protein ATP hydrolytic activity. II. Structure of the active site with ADP or ATP bound to wild type and mutant ATPase fragment. *J. Biol. Chem.*, **269**, 12899–12907.

Greengard,P. (1987) Neuronal phosphoproteins. *Mol. Neurobiol.*, **1**, 81–119.

Hayes,N.V., Bennett,A.F. and Baines,A.J. (1991) Selective Ca^{2+}-dependent interaction of calmodulin with the head domain of synapsin I. *Biochem. J.*, **275**, 93–97.

Herzberg,O., Chen,C.C.H., Kapadia,G., McGuire,M., Carroll,L.J., Noh,S.J. and Dunaway-Mariano,D. (1996) Swiveling-domain mechanism for enzymatic phosphotransfer between remote reaction sites. *Proc. Natl Acad. Sci. USA*, **93**, 2652–2657.

Holm,L. and Sander,C. (1993) Protein structure comparison by alignment of distance matrices. *J. Mol. Biol.*, **233**, 123–138.

Inui,M., Watanabe,T. and Sobue,K. (1994) Annexin VI binds to a synaptic vesicle protein, synapsin I. *J. Neurochem.*, **63**, 1917–1923.

Jones,T.A., Zou,J.-Y., Cowan,S.W. and Kjeldgaard,M. (1991) Improved methods for building protein models in electron density maps and the location of errors in these models. *Acta Crystallogr.*, **A47**, 110–119.

Kahn,D.W. and Besterman,J.M. (1991) Cytosolic rat brain synapsin I is a diacylglycerol kinase. *Proc. Natl Acad. Sci. USA*, **88**, 6137–6141.

Klagges,B.R.E. *et al*. (1996) Invertebrate synapsins: a single gene codes for several isoforms in *Drosophila*. *J. Neurosci.*, **16**, 3154–3165.

Kraulis,P.J. (1991) Molscript: a program to produce both detailed and schematic plots structures. *J. Appl. Crystallogr.*, **24**, 946–950.

Matsuda,K., Mizuguchi,K., Nishioka,T., Kato,H., Go,N. and Oda,J. (1996) Crystal structure of glutathione synthetase at optimal pH: domain architecture and structural similarity with other proteins. *Protein Eng.*, **9**, 1083–1092.

McPherson,P.S., Czernik,A.J., Chilcote,T.J., Onofri,F., Benfenati,F., Greengard,P., Schlessinger,J. and De Camilli,P. (1994) Interaction of Grb2 via its Src homology 3 domains with synaptic proteins including synapsin I. *Proc. Natl Acad. Sci. USA*, **91**, 6486–6490.

Mizutani,A., Tokumitsu,H. and Hidaka,H. (1992) Acidic calmodulin-binding protein, ACAMP-81, is MARCKS protein interacting with synapsin I. *Biochem. Biophys. Res. Commun.*, **182**, 1395–1401.

Murzin,A.G., Brenner,S.E., Hubbard,T. and Chothia,C. (1995) SCOP: a structural classification of proteins database for the investigation of sequences and structures. *J. Mol. Biol.*, **247**, 536–540.

Otwinowski,Z. (1991) Maximum likelihood refinement of heavy atom parameters. In Wolf,W., Evans,P.R. and Leslie,A.G.W. (eds), *Isomorphous Replacement and Anomalous Scattering. Proceedings of the CCP4 Study Weekend 25–26 January 1991*. SERC Daresbury Laboratory, Warrington, pp. 80–86.

Otwinowski,Z. and Minor,W. (1997) Processing of X-ray diffraction data collected in oscillation mode. *Methods Enzymol.*, **276**, 307–326.

Petrucci,T.C. and Morrow,J. (1997) Synapsin I: an actin-bundling protein under phosphorylation control. *J. Cell Biol.*, **105**, 1355–1363.

Rosahl,T.W., Geppert,M., Spillane,D., Herz,J., Hammer,R.E., Malenka,R.C. and Südhof,T.C. (1993) Short-term synaptic plasticity is altered in mice lacking synapsin I. *Cell*, **75**, 661–670.

Rosahl,T.W., Spillane,D., Missler,M., Herz,J., Selig,D.K., Wolff,J.R., Hammer,R.E., Malenka,R.C. and Südhof,T.C. (1995) Essential functions of synapsins I and II in synaptic vesicle regulation. *Nature*, **375**, 488–493.

Sriram,M., Osipiuk,J., Freeman,B.C., Morimoto,R.I. and Joachimiak,A. (1997) Human Hsp70 molecular chaperone binds two calcium ions within the ATPase domain. *Structure*, **5**, 403–414.

Steiner,J.P., Ling,E. and Bennett,V. (1987) Nearest neighbor analysis for brain synapsin I. Evidence for *in vitro* reassociation assays for association with membrane protein(s) and the M_r=68000 neurofilament subunit. *J. Biol. Chem.*, **262**, 905–914.

Südhof,T.C. (1995) The synaptic vesicle cycle: a cascade of protein–protein interactions. *Nature*, **375**, 645–653.

Südhof,T.C. *et al*. (1989) Synapsins: mosaics of shared and individual domains in a family of synaptic vesicle phosphoproteins. *Science*, **245**, 1474–1480.

Tanaka,T., Kato,H., Nishioka,T. and Oda,J. (1992) Mutational and proteolytic studies on a flexible loop in glutathione synthetase from *Escherichia coli* B: the loop and arginine 233 are critical for the catalytic reaction. *Biochemistry*, **31**, 2259–2265.

Waldrop,G.L., Rayment,I. and Holden,H.M. (1994) Three-dimensional structure of the biotin carboxylase subunit of acetyl-CoA carboxylase. *Biochemistry*, **33**, 10249–10256.

Wang,C.-R., Esser,L., Smagula,C.S., Südhof,T.C. and Deisenhofer,J. (1997) Identification, expression, and crystallization of the protease-resistant conserved domain of synapsin I. *Protein Sci.*, **6**, 2264–2267.

Wolodko,W.T., Fraser,M.E., James,M.N.G. and Bridger,W.A. (1994) The crystal structure of succinyl-CoA synthetase from *Escherichia coli* at 2.5-Å resolution. *J. Biol. Chem.*, **269**, 10883–10890.

Yamaguchi,H., Kato,H., Hata,Y., Nishioka,T., Kimura,A., Oda,J. and Katsube,Y. (1993) Three-dimensional structure of the glutathione synthetase from *Escherichia coli* B at 2.0 Å resolution. *J. Mol. Biol.*, **229**, 1083–1100.

Received October 16, 1997; revised November 28, 1997; accepted December 1, 1997